BMC Genomics

RESEARCH

Open Access

Transcriptomic profiling reveals the complex interaction between a bipartite begomovirus and a cucurbitaceous host plant

Wen-Ze He[1†], Li Zhao[2†], Kai Sun[3], Zhen Feng[1], Gen Zhou[1] and Qiong Rao[1*]

Abstract

Background Begomoviruses are major constraint in the production of many crops. Upon infection, begomoviruses may substantially modulate plant biological processes. While how monopartite begomoviruses interact with their plant hosts has been investigated extensively, bipartite begomoviruses-plant interactions are understudied. Moreover, as one of the major groups of hosts, cucurbitaceous plants have been seldom examined in the interaction with begomoviruses.

Results We profiled the zucchini transcriptomic changes induced by a bipartite begomovirus squash leaf curl China virus (SLCCNV). We identified 2275 differentially-expressed genes (DEGs), of which 1310 were upregulated and 965 were downregulated. KEGG enrichment analysis of the DEGs revealed that many pathways related to primary and secondary metabolisms were enriched. qRT-PCR verified the transcriptional changes of twelve selected DEGs induced by SLCCNV infection. Close examination revealed that the expression levels of all the DEGs of the pathway Photosynthesis were downregulated upon SLCCNV infection. Most DEGs in the pathway Plant-pathogen interaction were upregulated, including some positive regulators of plant defenses. Moreover, the majority of DEGs in the MAPK signaling pathway-plant were upregulated.

Conclusion Our findings indicates that SLCCNV actively interact with its cucurbitaceous plant host by suppressing the conversion of light energy to chemical energy and inducing immune responses. Our study not only provides new insights into the interactions between begomoviruses and host plants, but also adds to our knowledge on virus-plant interactions in general.

Keywords Transcriptional reprograming, Plant-virus interaction, Bipartite begomovirus, *Cucurbita pepo*, Squash leaf curl China virus

†Wen-Ze He and Li Zhao contributed equally to this work.

*Correspondence:
Qiong Rao
qiong.rao@zafu.edu.cn
[1]Zhejiang Key Laboratory of Biology and Ecological Regulation of Crop Pathogens and Insects, Zhejiang A&F University, Hangzhou 311300, China
[2]Hangzhou Agricultural Technology Extension Center, Hangzhou 310058, China
[3]Zhejiang Provincial Key Laboratory of Biometrology and Inspection & Quarantine, College of Life Sciences, China Jiliang University, Hangzhou 310018, China

Background

Plant viral pathogens are the major constraints in agriculture [1]. As a group of obligate parasites, viruses actively interact with their plant hosts during infection. On the one hand, viruses may significantly modulate plant physiology so as to create microenvironment conducive to virus replication [2]. On the other hand, plant hosts may deploy a repertoire of defenses responses to restrict excessive virus multiplication and secure their own survival [3]. Together, these intimate interactions dramatically alter plant physiology [3]. Understanding these molecular interactions is instrumental in dissecting viral pathogenesis within plant hosts and will in turn promote the control of viral diseases [4].

Begomoviruses (family *Geminiviridae*) are a group of DNA viruses that infect many economically important crops [5]. Under natural conditions, begomoviruses are transmitted by *Bemisia tabaci* sensu lato, a species complex consisting of more than 40 cryptic species [6, 7]. Begomoviruses can be monopartite or bipartite depending on the number of genomic molecules [8]. While the genomes of bipartite begomoviruses consist of two DNA molecules designated as DNA-A and DNA-B, monopartite begomoviruses have only one genomic molecule resembling the DNA-A component of bipartite begomoviruses [8–11]. In the last decades, the economic significance of begomoviruses in crop production has sparked extensive investigations on the interactions between begomoviruses and their plant hosts [10, 11]. These studies mostly focused on the functional characterization of viral and plant proteins and overall plant responses such as transcriptomic changes induced by begomoviruses [9–22]. It should be noted, however, most studies on plant transcriptional reprograming induced by begomoviruses works on monopartite begomoviruses such as tomato yellow leaf curl virus and chilli leaf curl virus [12–22]. More importantly, only a limited number of plants have been examined such as tomato, pepper, *Arabidopsis thaliana*, *Nicotiana benthamiana* and cassava. How the other groups of hosts such as plants in the family *Cucurbitaceae* respond to begomovirus infection remains enigmatic.

Initially identified on pumpkin plants, squash leaf curl China virus (SLCCNV) was later found to infect a variety of cucurbitaceous crops including melon and zucchini, leading to considerable economic losses [23, 24]. Recently, new hosts of SLCCNV such as tomato were identified [25]. In China, SLCCNV has been found in many provinces including Guangxi, Hainan and Shandong [24–26]. This virus has also been identified in many South and Southeast Asian countries such as Pakistan, India, Malaysia and Philippines [23, 27, 28]. SLCCNV has emerged as one of the key factors that threaten the production of many cucurbitaceous crops in many regions in Asia [23, 24, 29]. While the economic significance of SLCCNV has been widely recognized, its biology is understudied especially in interaction with cucurbitaceous plants. Advances in the understanding of molecular SLCCNV-cucurbitaceous plant interactions will provide important reference for improving plant defenses against this emerging pathogen.

Given the current state of knowledge of and the ongoing challenges posed by SLCCNV, there is an urgent need to elucidate the molecular interactions between SLCCNV and its cucurbitaceous hosts. In this study, we profiled the transcriptome of zucchini plants in response to SLCCNV infection. By examining the genes whose expressions were affected, we uncovered the intricate interplays between SLCCNV and its cucurbitaceous plant hosts. Our findings contribute to a better understanding of begomovirus-cucurbitaceous plant interactions and virus-plant interactions in general.

Methods

Plant and virus

Cucurbita pepo cv. Faguodongkui was used. Plants were cultivated in an insect-proof greenhouse under natural lighting and maintained at 25±3 °C. Agro-inoculation was conducted when zucchini plants reached one or two true-leaf stage. For virus, SLCCNV isolate Guangxi2017 was used. The GenBank accession codes for DNA-A and DNA-B were MG525551 and MG525552, respectively. Agroinoculation was conducted as described before [26]. Agrobacteria containing the infectious clones of DNA-A and DNA-B were cultured separately until OD600 reached 2.0. Agrobacteria were centrifuged and resuspended in equal volume (20 mL) of resuspension buffer (10 mM $MgCl_2$, 10 mM MES and 200 μM acetosyringone). Equal volume (20 mL) of agrobacteria solutions containing infectious clones of DNA-A and DNA-B were mixed. Next, 1 mL syringe was utilized to inoculate the agrobacteria mixture into both the true leaves and cotyledons of zucchini plants. Four weeks post agroinoculation, plants were sampled for transcriptomic analysis after visual inspection of virus infection symptoms (Fig. 1) and PCR detection of SLCCNV DNA-A. DNA was extracted from the first fully-expanded leaves using Plant Genomic DNA Kit (Tiangen, China) and subjected to PCR with primers listed in Table S1.

RNA extraction, library preparation and sequencing

The top fully-expanded leaves were harvested and leaves from two plants were mixed as one sample. Four samples were analyzed for both pBINPLUS and SLCCNV treatments. Total RNA was extracted using TRIzol (Ambion, USA) as per the manual. RNA quality and quantity were determined using Nanodrop2000 and Agilent5300. RNA samples that have a concentration ≥ 30 ng/μL, RQN > 6.5,

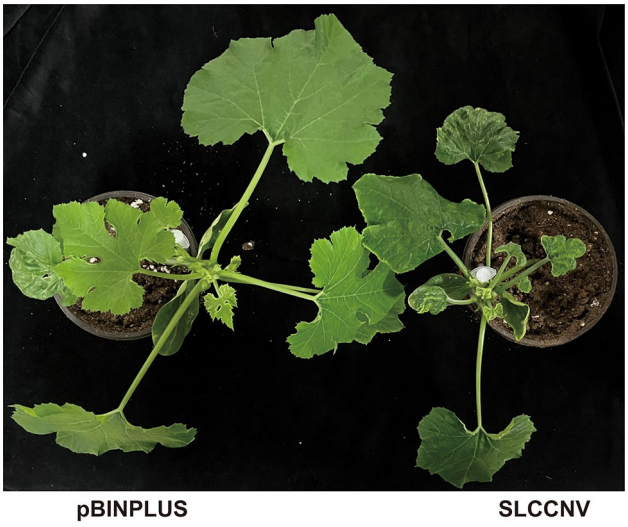

Fig. 1 Symptoms induced by SLCCNV in zucchini plants. Zucchini plants were inoculated with pBINPLUS (empty vector) or SLCCNV DNA-A + DNA-B. Symptoms of SLCCNV infection in zucchini plants showed dwarf, downward leaf curl and mosaic in young leaves and mosaic in old leaves. Pictures were taken at four weeks post inoculation

and an OD260/280 ratio between 1.8 and 2.2 were used for following analysis. mRNA isolation was conducted with Oligo dT magnetic beads. The isolated mRNA was randomly fragmented into pieces of around 300 bp using a fragmentation buffer. First-strand cDNA was synthesized using random primers, followed by second-strand synthesis to create double-stranded cDNA. Blunt ends were created in the cDNA ends and a base was added to the 3' end, and then adapters for sequencing were added. Adapter-ligated cDNAs were purified and amplified using PCR. The obtained library was quantified with Qubit 4.0 and sequenced on the NovaSeq X Plus platform.

Quality control and mapping of reads

Adapter sequences, low-quality reads, sequences with a high rate of 'N' bases (uncertain base information) and short sequences in the raw sequencing data were removed by filtering the original sequencing data using the software fastp with its default parameters. The steps were as follows: (1) remove adapter sequences from the reads and eliminate reads that lack an insert fragment due to adapter self-ligation or other reasons; (2) Trim low-quality bases (<20) at the 3' end of the sequences. If there are still bases with a quality value less than 10 in the sequence, discard the entire sequence; otherwise, retain it; (3) Remove reads with an 'N' content rate exceeding 10%; (4) Discard sequences shorter than 20 bp after adapter removal and quality trimming. After quality control, data quality including the distribution of base error rates and base content was re-assessed. Clean reads were aligned with the reference genome of *C. pepo* (MU-CU-16, http://cucurbitgenomics.org/v2/organism/4) to obtain mapped reads for subsequent transcript assembly and expression level analysis. Alignment details such as gene coverage, distribution of reads across different regions of the reference genome and distribution across various chromosomes were assessed.

Identification of differentially-expressed genes (DEGs)

Gene expression levels were quantitatively analyzed so as to identify differentially-expressed genes (DEGs) between treatments. The read counts of each gene were obtained using the results of comparison to the *C. pepo* genome (MU-CU-16, http://cucurbitgenomics.org/v2/organism/4). Read counts were converted to FPKM, and then the standardized gene expression levels were obtained. To identify genes that were differentially expressed between treatments, the software DESeq2 was used and the default criteria for identifying DEGs were: a False Discovery Rate (FDR) less than 0.05 and an absolute log2 Fold Change (|log2FC|) greater than or equal to 1. A gene was considered a DEG when it met both criteria.

Functional annotation and enrichment of DEGs

KEGG is a knowledge base for systematic analysis of gene function, linkage genomic information and functional information. Functional annotation of DEGs was conducted using KEGG database (http://www.genome.jp/kegg/) Version 2022.10. KEGG functional enrichment analysis of DEGs was conducted to identify over-represented biological processes, molecular functions, and cellular components, as well as to uncover significant pathways involved. The KEGG pathway enrichment analysis was performed using R-script to identify pathways. The analysis was based on the Fisher's exact test, with a threshold of adjusted $P<0.05$ to denote statistical significance for enriched KEGG terms.

Quantitative reverse transcription PCR (qRT-PCR)

Total RNAs were extracted from samples using TRIzol, and reverse-transcribed using Evo M-MLV RT Kit with gDNA Clean for qPCR (Accurate Biology, China). Quantitative PCR (qPCR) analysis was performed using SYBR Green Premix Pro Taq HS qPCR Kit (Accurate Biology, China) and CFX96 Real Time PCR Detection System (Bio-Rad, USA). Primers are listed in Table S1. *β-tubulin* (tubulin beta chain, Cp4.1LG00g13540) was used as a reference gene because it was stably expressed in samples from the two treatments (Table S3). Each sample was set up with two technical replicates. The procedure was as follows: initial denaturation at 95 °C (30 s), followed by 40 cycles of denaturation at 95 °C (5 s), annealing and extension at 60 °C (34 s), with a melting curve included to assess primer specificity. Real time data were calculated using $2^{-\triangle\triangle Ct}$ as normalized to zucchini *β-tubulin* and pBINPLUS control.

Results

Symptom of SLCCNV infection in zucchini plants

At four weeks post inoculation, PCR was performed to examine the presence of SLCCNV genomic DNA in pBINPLUS-inoculated and SLCCNV-inoculated zucchini plants. SLCCNV DNA-A can be readily amplified in SLCCNV DNA-A+DNA-B-inoculated zucchini plants, but not in pBINPLUS-inoculated plants (Fig. S1). As for symptoms, the leaves of SLCCNV-infected plants were much smaller than that of control. SLCCNV induced downward leaf curl and mosaic in young leaves and mosaic in old leaves. Additionally, old zucchini leaves became dark green and their thickness increased upon SLCCNV infection (Fig. 1).

Transcriptomic analysis and genome mapping

Eight samples were subjected to transcriptome sequencing, with four samples for both pBINPLUS and SLCCNV treatments. For each sample, we obtained 42,320,894–52,936,382 raw reads and 6,390,454,994–7,993,393,682 raw bases. After data filtering, 42,027,984–52,532,140 clean reads and 6,304,709,668–7,829,817,814 clean bases were obtained for each of the samples. The base error rates were below 0.013%. Q20 and Q30 values were over 98% and 96%, respectively. The GC content was 46.11–47.55% (Table S2). Out of the 55,620 transcripts detected, almost half (26110, 46.9%) were over 1800 bp, and 4177 transcripts were between 1601 and 1800 bp, 4233 transcripts were between 1401 and 1600 bp, 4250 transcripts were between 1201 and 1400 bp, 4062 transcripts were between 1001 and 1200 bp (Fig. S2). It is thus clear that the quantity and quality of the RNA-Seq data were sufficient for subsequent analysis. Clean data were mapped to the reference genome. The rates of successful mapping were 96.39–97.32%. The majority of clean reads (90.99–91.88%) were singly mapped to the genome (Table S3).

Identification and functional annotation of DEGs

Gene expression analysis revealed that when compared to pBINPLUS, SLCCNV infection upregulated the expression levels of 1310 genes and downregulated that of 965 genes in zucchini plants (Fig. 2). These DEGs were functionally annotated using KEGG database. In total, 751 DEGs were annotated and further sorted into 18 unique pathway groups. These pathways spanned across five major pathway categories, namely Metabolism, Genetic

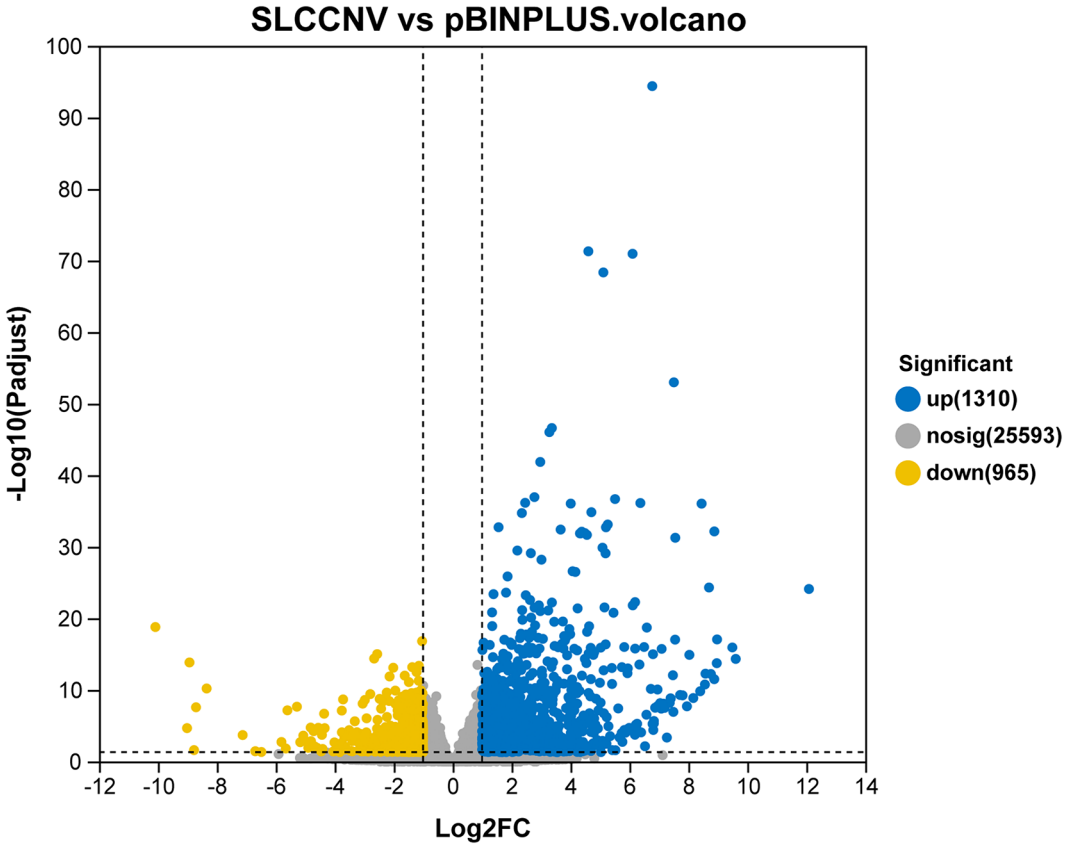

Fig. 2 Volcano plot of DEG analysis between pBINPLUS and SLCCNV treatments. Each point in the plot corresponds to a specific gene. Blue points (right side) indicate significantly upregulated genes, yellow points (left side) represent significantly downregulated genes, and gray points (middle) signify genes with no significant differences. The closer a point is to the edges and the top of the plot, the more pronounced its expression difference

Information Processing, Environmental Information Processing, Cellular Processes, and Organismal Systems. A notable predominance was observed within the pathway group Metabolism, with the pathways Carbohydrate metabolism, Energy metabolism, and Amino acid metabolism containing the highest number of DEGs (Fig. S3). Conversely, the pathway groups Cellular Processes and Organismal Systems were relatively less represented, with only a handful of DEGs identified within these categories.

Functional enrichment of DEGs

To examine the biological processes regulated by DEGs, an enrichment analysis was conducted using the KEGG database. DEGs were found to regulate various pathways, and the top 20 most significantly enriched pathways were identified (Table S5, Fig. 3). Of these pathways, Photosynthesis stood out as the most significantly enriched, and two related pathways Photosynthesis-antenna proteins and Carbon fixation in photosynthetic organisms were similarly enriched. Notably, many primary and secondary metabolism pathways were enriched, including Glyoxylate and dicarboxylate metabolism, Porphyrin metabolism, Nitrogen metabolism, among others. Two pathways that were of particular relevance to plant-virus interaction were identified, namely Plant-pathogen interaction and MAPK signaling pathway-plant. Three pathways were subjected to further analysis, namely Photosynthesis, Plant-pathogen interaction and MAPK signaling pathway-plant.

qRT-PCR verification of the expression of DEGs

Prior to further analysis of enriched pathways, we conducted qRT-PCR to verify the expression of DEGs. We selected twelve DEGs with four from each of the three pathways Photosynthesis, Plant-pathogen interaction and MAPK signaling pathway-plant. The changes in the expression levels of these DEGs were most pronounced in the three pathways. Transcriptomic analysis revealed that the expression of all the four DEGs from the pathway Photosynthesis (Cp4.1LG04g03330, Cp4.1LG19g12170, Cp4.1LG01g20490 and Cp4.1LG13g04750) were downregulated by SLCCNV (SLCCNV vs. pBINPLUS fold change < 1). Similarly, in qRT-PCR their expression was downregulated (SLCCNV vs. pBINPLUS fold change < 1), verifying RNA-seq data (Fig. 4A-D). Additionally, the changes in the expression of DEGs in the pathways

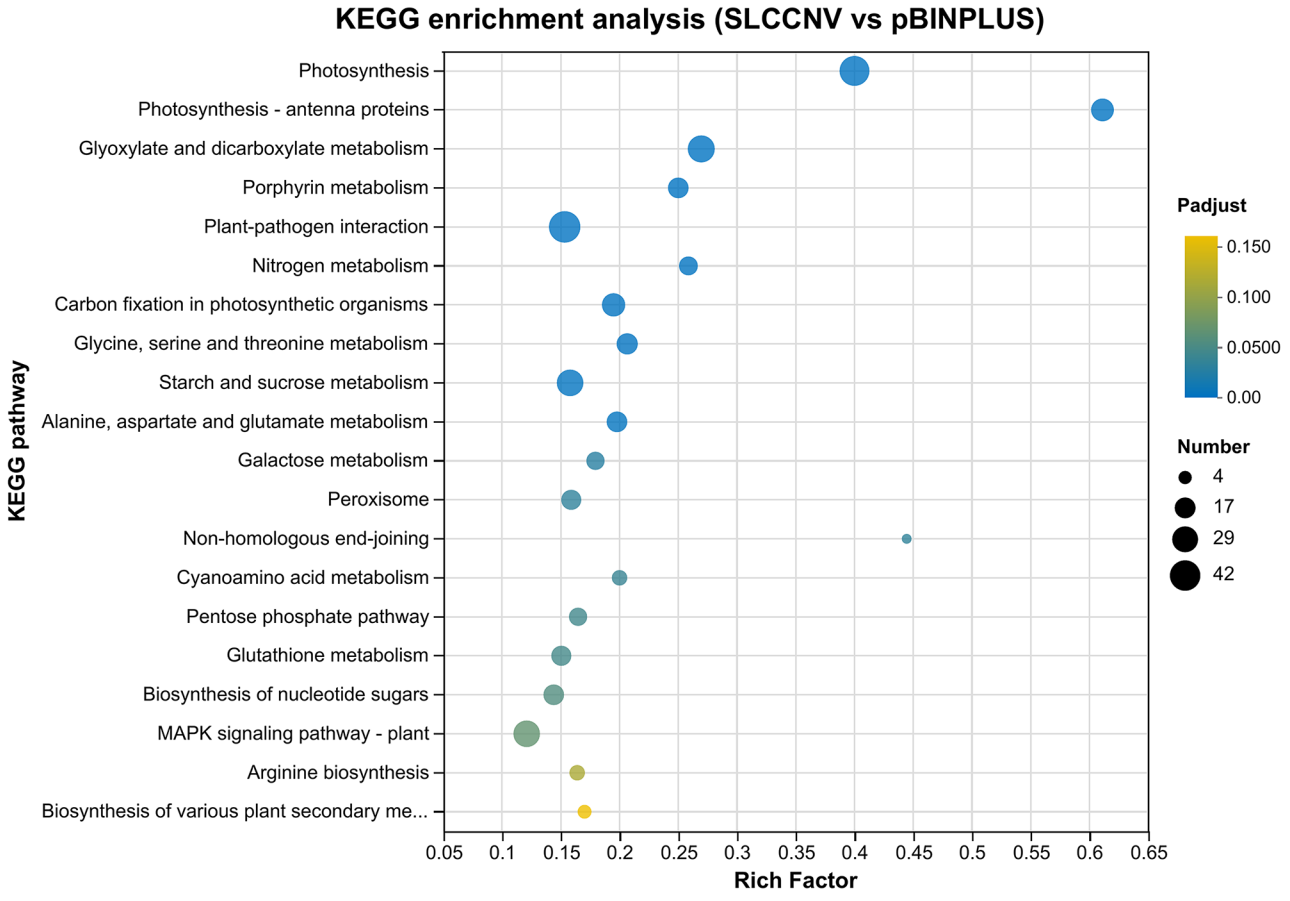

Fig. 3 Distribution of the top 20 enriched KEGG pathways. The Y-axis represented the name of the pathway, and the X-axis indicated the rich factor of the pathway. The q value was indicated by the color of the dots, and the number of genes in each pathway was indicated by the size of the dots

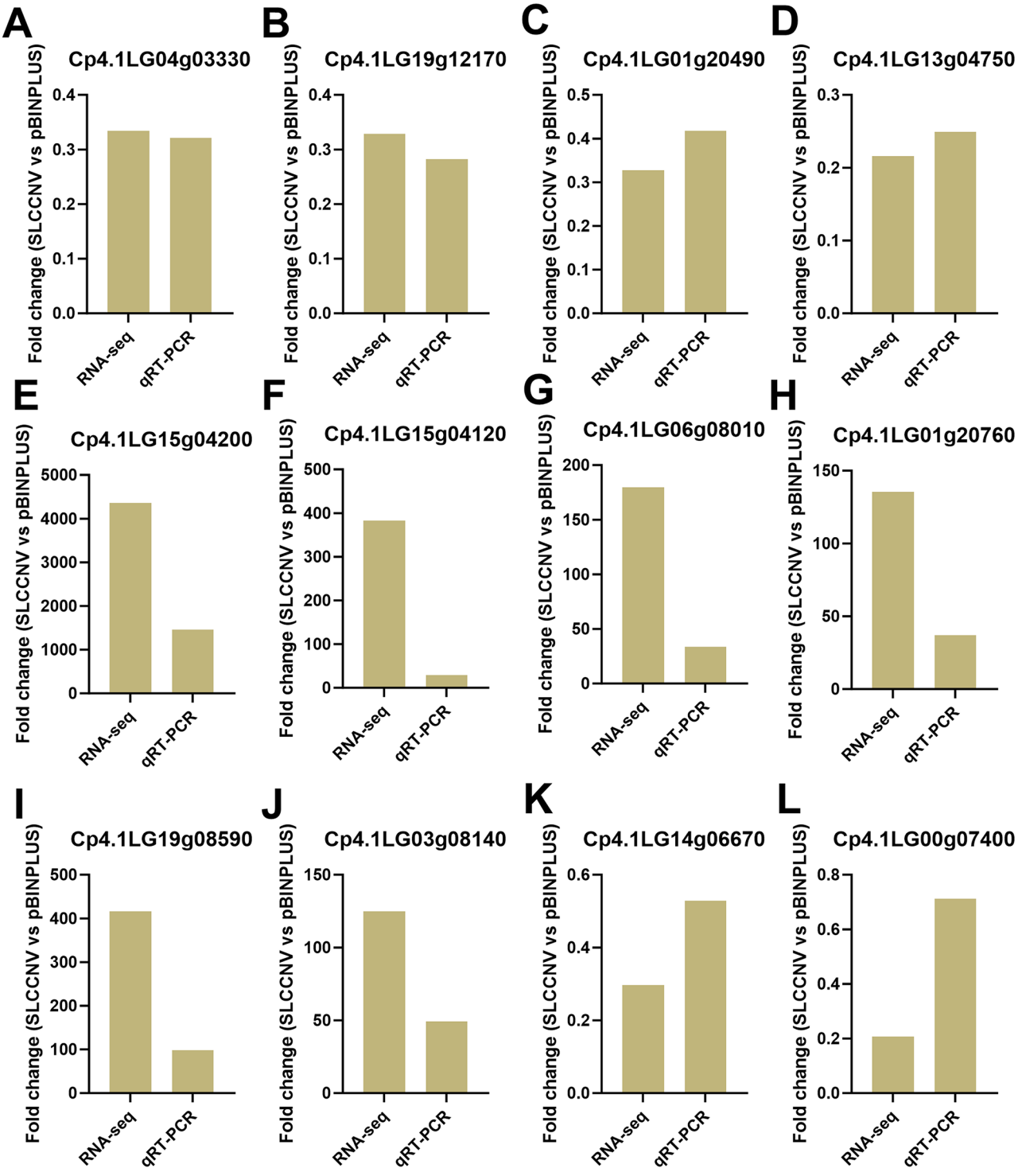

Fig. 4 qRT-PCR validation of the fold change (SLCCNV vs. pBINPLUS) of DEGs. (**A**-**D**) DEGs in the pathway Photosynthesis; (**E**-**H**) DEGs in the pathway Plant-pathogen interaction; (**I**-**L**) DEGs in the pathway MAPK signaling pathway-plant. The number of replicates was 4 for RNA-seq, 5–6 for qRT-PCR

Plant-pathogen interaction and MAPK signaling pathway-plant induced by SLLCNV were consistent in RNA-seq and qRT-PCR data (Fig. 4E-L). These findings suggest that DEGs obtained in our transcriptomic analysis were reliable and can be used for further analysis.

Photosynthesis

Photosynthesis was the most significantly enriched pathway, with a rich factor and an adjusted *P* value of 0.4 and 2.52E-16, respectively (Table S5). Notably, the expression of all the 38 DEGs in this pathway were

downregulated (Table S6). The expression level of these DEGs in SLCCNV-infected plants were 21.6–48.4% of that in control plants. For example, the expression of two genes encoding photosystem II 22 kDa protein (PsbS homology) was downregulated by 67.3% and 78.4%, respectively. The expression of *photosystem I reaction center subunit N* (*PsaN* homology) and *Cytochrome b6-f complex iron-sulfur subunit* (*PetC* homology) was downregulated by 67.1% and 66.6%, respectively. Summary of the DEGs in the pathway Photosynthesis revealed that all the components of photosynthesis complex were affected by SLCCNV infection (Fig. 5). Specifically, the expression levels of the homologs of PsbO, PsbP, PsbQ, PsbR, PsbS, PsbW, and Psb27 in photosystem II were downregulated. For photosystem I, the expression levels of the homologs of PsaD, PsaE, PsaF, PsaG, PsaH, PsaL, PsaN and PsaO were downregulated. The expression levels of *PetC* (cytochrome b6/f complex) homolog, and *PetE*, *PetF* and *PetH* that were involved in photosynthethic electron transport were downregulated. Also downregulated were the expression levels of the genes encoding F-type ATPase gamma, delta and b.

Plant-pathogen interaction

Plant-pathogen interaction was the top fifth significantly enriched pathway, with a rich factor and an adjusted *P* value of 0.15 and 0.00035, respectively (Table S5). The expression levels of the majority of the 42 DEGs in this pathway were upregulated (Table S7). The expression levels of the 36 upregulated DEGs in SLCCNV-infected plants were 2.05-4360.84 folds of that in control plants. For the six downregulated DEGs, their expression levels in plants were reduced by 51.3–74.5% upon SLCCNV infection. Summary of the DEGs in the pathway Plant-pathogen interaction revealed that many plant defense machineries were affected by SLCCNV infection (Fig. 6). Specifically, the expression levels of the homologs of *CDPK*, *Rboh* and *CNGCs* that regulated pathogen-associated molecular pattern (PAMP)-triggered immunity increased upon SLCCNV infection. Similarly, the expression levels of the homologs of *MPK4*, *WRKY25/33*,

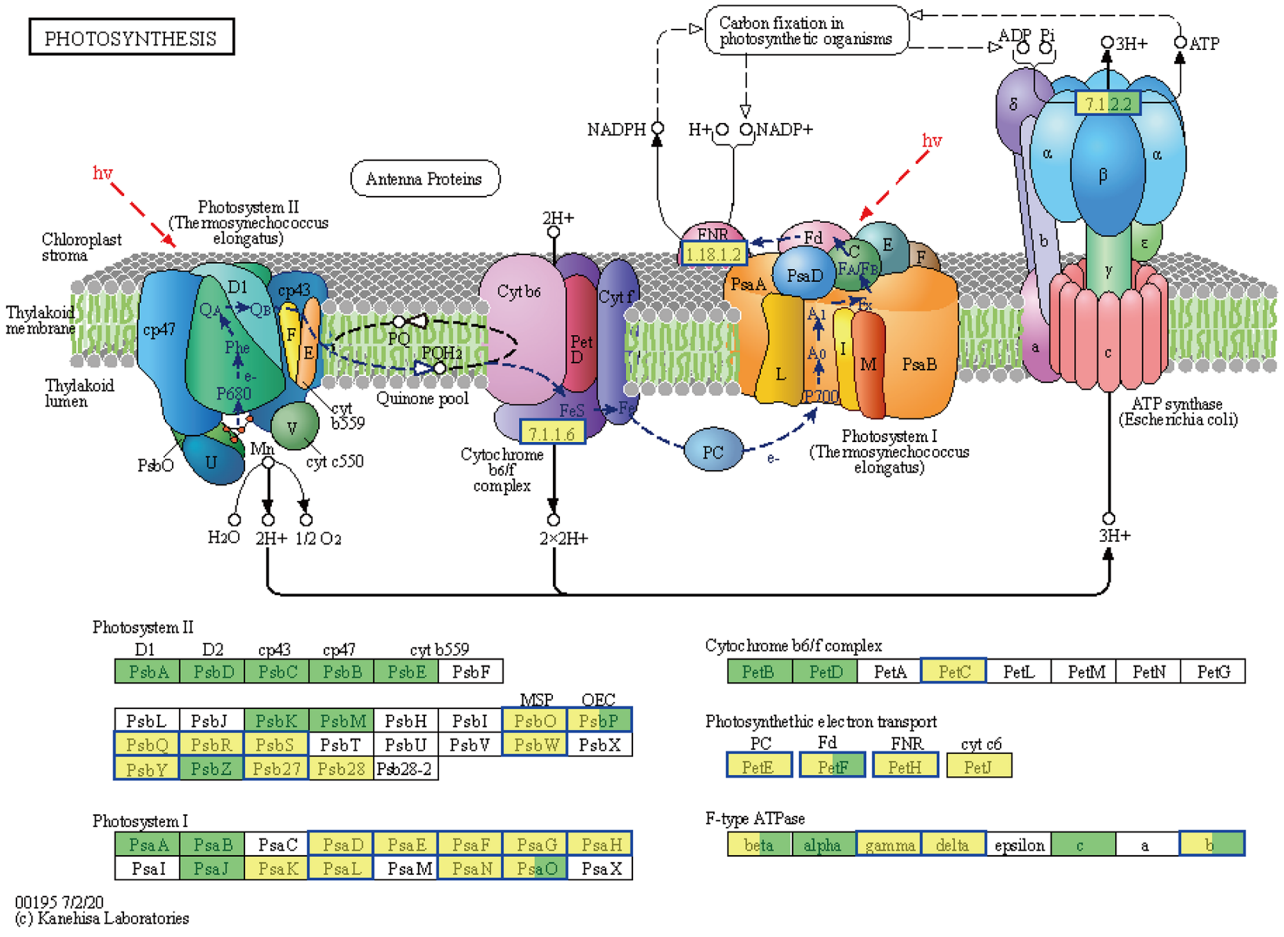

Fig. 5 Regulation of the expression of DEGs in photosynthesis pathway. The photosynthetic cascade is shown, followed by the list of important components. For each component, blue frames indicate downregulation of gene expression upon SLCCNV infection. Yellow fill-ins of the box indicate previously-identified transcripts, while green fill-ins indicate newly-found transcripts

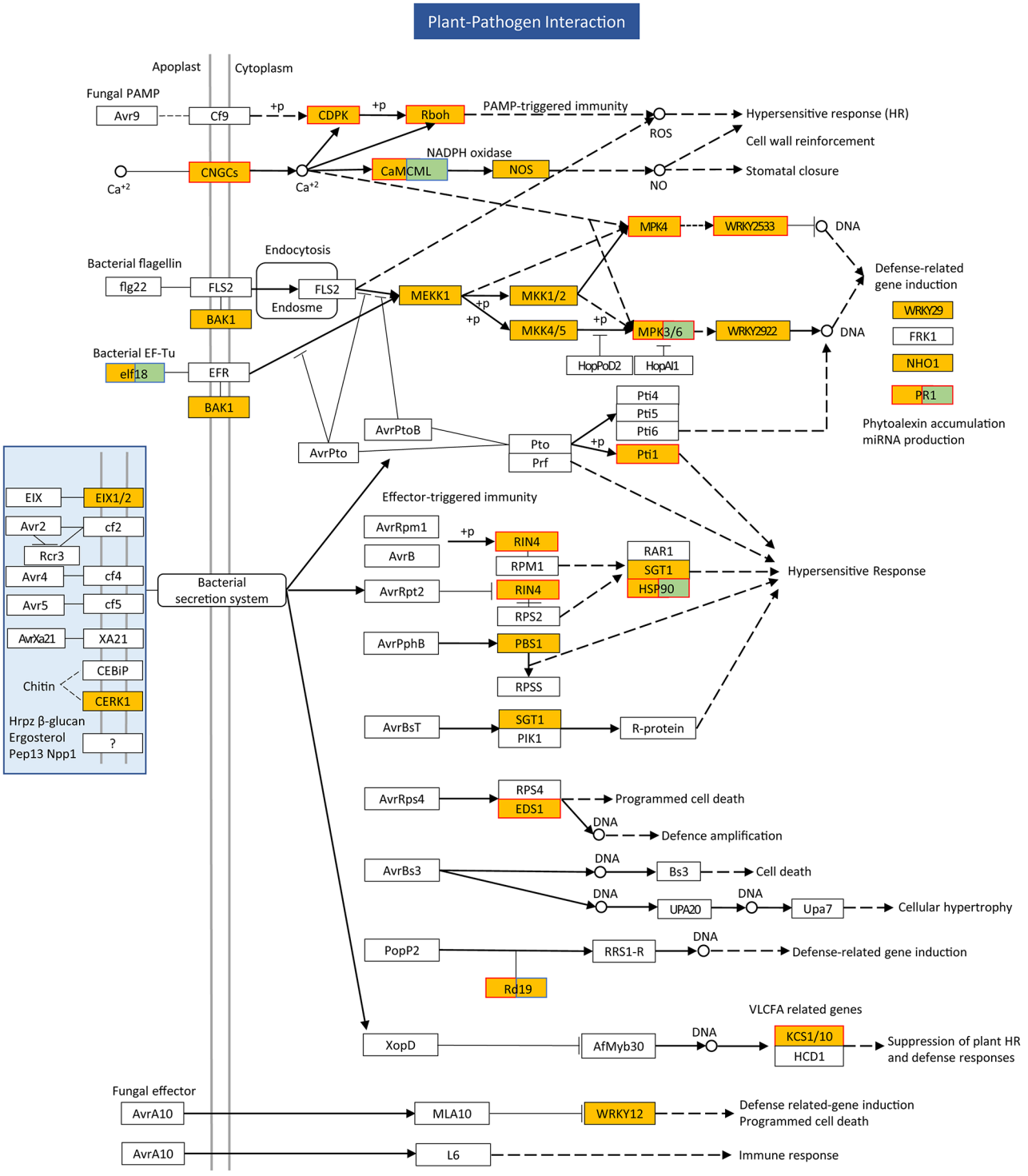

Fig. 6 Regulation of the expression of DEGs in plant-pathogen interaction pathway. The signaling cascade is shown with the important components involved. For each component, blue and red frames indicate downregulation and upregulation of gene expression, respectively. Yellow fill-ins of the box indicate previously-identified transcripts, while green fill-ins indicate newly-found transcripts

MPK3/6 and *PR1* regulating defense-related gene induction were upregulated. In addition, the expression of the homologs of *Pti1*, *RIN4* and *HSP90* that regulated hypersensitive responses and *EDS1* that regulated programmed cell death was induced by SLCCNV.

MAPK signaling pathway-plant

MAPK signaling pathway-plant was the top eighteenth significantly enriched pathway, with a rich factor and an adjusted *P* value of 0.12 and 0.063, respectively (Table S5). Of the 30 DEGs in this pathway, the expression levels of 24 and six DEGs were upregulated and downregulated, respectively (Table S8). The expression levels of the 24 upregulated DEGs in SLCCNV-infected plants were 2.028-4360.84 folds of that in control plants. For the six downregulated DEGs, their expression levels in plants were reduced by 52.9–79.3% upon SLCCNV infection. Summary of the DEGs in this pathway revealed that many plant defenses were modulated by SLCCNV infection (Fig. 7). For example, the expression levels of the homologs of *MPK4* and *WRKY33* regulating camalexin synthesis increased upon SLCCNV infection. Similarly, the expression levels of the homologs of *MPK3/6* and *PR1* that regulated late defense response for pathogen were upregulated. The expression of the homologs of *MKK9*, *MPK3/6*, *EIN3/EIL*, *ERF1* and *CHiB* that were involved in defense response were induced by SLCCNV.

Discussion

Begomovirus-plant interactions have been extensively studied in the past decades, yet how bipartite begomoviruses interact with cucurbitaceous host plants remain unknown. To address this knowledge gap, we first phenotypically characterized SLCCNV infection in zucchini plants (Fig. 1) and then profiled zucchini transcriptomic changes induced by SLCCNV. Quality control analysis revealed that the quantity and quality of RNA-seq data were sufficient for further analysis (Fig. S1, Table S2-S3). Gene expression analysis identified more than 2000 DEGs, which were subjected to KEGG enrichment analysis (Figs. 2 and 3, Table S4-S5). qRT-PCR verified the expression of DEGs in three selected KEGG pathways (Fig. 4). Finally, we focused on three KEGG pathway that were of particular relevance to virus-plant interaction, including Photosynthesis, Plant-pathogen interaction and MAPK signaling pathway-plant (Figs. 5, 6 and 7, Table S6-S8).

Previously, studies on SLCCNV focus on its detection and sequence analysis in field-collected samples [23–25, 27–29], or its interaction with whitefly vectors [26]. How SLCCNV interact with its cucurbitaceous host plants remain hitherto uncharacterized. Here we used transcriptomic analysis to profile zucchini gene transcriptional changes induced by SLCCNV. Transcriptome sequencing offers a powerful tool for exploring complex biotic interactions and has been used extensively in begomovirus-plant interactions [12–22]. By clarifying the gene expression profiles in virus-infected and control plants, transcriptomic analysis can provide unprecedented insights into the complex molecular dialogue between plants and viruses. These molecular dialogues are crucial for understanding the interaction between plant hosts and viruses, a group of notorious pathogens [30, 31]. In this study, for the first time, we profiled the transcriptomic changes induced by SLCCNV in zucchini plants, and unraveled many important factors potentially involved in SLCCNV-zucchini interactions.

Photosynthesis is arguably the most important biological processes on earth that directly or indirectly provide energy to almost all forms of life [32]. The photosynthetic apparatus in plants includes photosystem II, photosystem I, cytochrome b6/f complex, photosynthethic electron transport pathways and ATPase [32]. Photosynthesis is often targeted by plant viruses, leading the development of symptoms such as mosaic [2]. In this study, we found all major photosynthetic components were disrupted by SLCCNV. This disruption may be largely responsible for the development of SLCCNV-induced symptoms, for example leaf mosaic due to reduced chloroplast activity and dwarf due to reduced energy assimilation. The disruption of photosynthesis pathway has also been uncovered in other plant-begomovirus pathosystems including cassava-African cassava mosaic virus, chilli and chilli leaf curl virus, among others [16, 33], suggesting the conserved targeting of plant photosynthesis pathway by begomoviruses. Additionally, a recent report unraveled the contribution of photosynthesis-related genes including *PsaC* from photosystem I and *ATP-synthase α-subuni*t (*ATPsyn-α*) to plant antiviral defenses [34]. The disruption of photosynthetic apparatus found in our study may also be associated with the interference of plant defense machinery by SLCCNV.

Upon invasion of pathogens, plant mounts a repertoire of defense machineries to sustain their own survival. The perception of PAMPs by plants triggers PAMP-triggered immunity; as countermeasures, pathogens suppress PAMP-triggered immunity by deploying effectors, which are often recognized by plants and induce effector-triggered immunity [35]. In this study, we found that the expression levels of many genes in several PAMP-triggered immunity pathways were upregulated upon SLCCNV infection. Similarly, the expression of a handful of genes in effector-triggered immunity in zucchini plants was induced by SLCCNV. Mitogen-activated protein kinase (MAPK) cascade is a central signaling pathway that connect pathogen perception with downstream immune responses [35, 36]. MAPK is involved in the regulation of various phytohormone pathways and

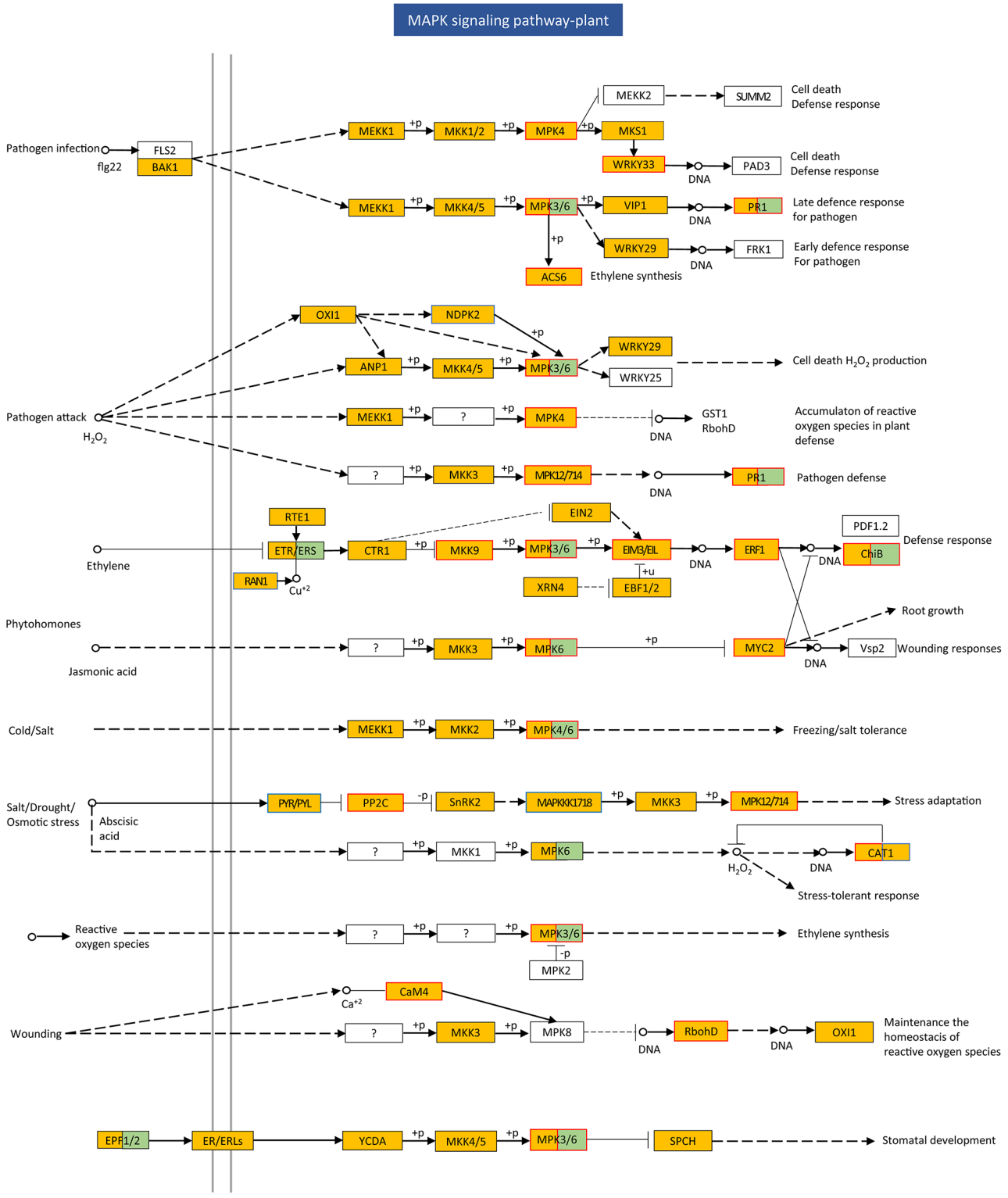

Fig. 7 Regulation of the expression of DEGs in MAPK signaling pathway-plant. The signaling cascade is shown with the important components involved. For each component, blue and red frames indicate downregulation and upregulation of gene expression, respectively. Yellow fill-ins of the box indicate previously-identified transcripts, while green fill-ins indicate newly-found transcripts

plant responses to abiotic stresses [36]. Here we found that the expression levels of many components of MAPK cascade were upregulated upon SLCCNV infection. Specifically, the expression levels of many MAPK components involved in the regulation of pathogen infection and attack, phytohormone pathways including ethylene, jasmonic acid and abscisic acid, and plant responses to ozone and wounding were upregulated. For example, the expression of *MKK9* and *MPK3/6* regulating ethylene signaling pathways and *MPK6* regulating jasmonic acid signaling pathway was induced by SLCCNV. The upregulation of genes regulating two layers of plant immunity and MAPK signaling pathway suggests the activation of plant immune machineries upon SLCCNV infection.

Conclusions

To sum up, here we have profiled the changes in gene expression in a cucurbitaceous host plant upon the infection of a bipartite begomovirus. SLCCNV modulated the expression of over 2000 genes, indicating dramatic modification of zucchini biology. More specifically, SLCCNV suppressed the expression of many genes involved in zucchini photosynthesis, likely contributing to the development of virus infection symptom. The expression of many genes regulating plant defenses was induced by SLCCNV, suggesting the activation of plant immune system. Our findings reveal the intimate interaction between a cucurbitaceous host and a bipartite begomovirus that will be instrumental in advancing our understanding of plant-begomovirus interaction and plant-virus interaction in general.

Supplementary Information

The online version contains supplementary material available at https://doi.org/10.1186/s12864-024-10781-6.

Supplementary Material 1
Supplementary Material 2
Supplementary Material 3
Supplementary Material 4
Supplementary Material 5
Supplementary Material 6
Supplementary Material 7
Supplementary Material 8
Supplementary Material 9
Supplementary Material 10

Author contributions

W.Z.H and Q.R conceived and designed research. L.Z and K.S conducted experiments. Z.F and G.Z analyzed data. W.Z.H wrote the manuscript. Q.R revised the manuscript. All authors read and approved the manuscript.

Funding

Financial support for this study was provided by Scientific Research and Development Fund Project of Zhejiang Agriculture and Forestry University (2023LFR070) and Zhejiang Provincial Natural Science Foundation (No. LQ22C140003).

Data availability

The raw data of RNA-seq were deposited in Sequence Read Archive database under the project number PRJNA1131561.

Declarations

Ethics approval and consent to participate

Not applicable.

Consent for publication

Not applicable.

Competing interests

The authors declare no competing interests.

Received: 8 July 2024 / Accepted: 9 September 2024
Published online: 18 September 2024

References

1. Tatineni S, Hein GL. Plant viruses of agricultural importance: current and future perspectives of virus disease management strategies. Phytopathol. 2023;113:117–41.
2. Osterbaan LJ, Fuchs M. Dynamic interactions between plant viruses and their hosts for symptom development. J Plant Pathol. 2019;101:885–95.
3. Ye J, Zhang LL, Zhang X, Wu XJ, Fang RX. Plant defense networks against insect-borne pathogens. Trends Plant Sci. 2021;26(3):272–87.
4. Rubio L, Galipienso L, Ferriol I. Detection of plant viruses and disease management: relevance of genetic diversity and evolution. Front Plant Sci. 2020;11:1092.
5. Fiallo-Olivé E, Navas-Castillo J, Begomoviruses. What is the secret(s) of their success? Trends Plant Sci. 2023;28:715–27.
6. Wang XW, Blanc S. Insect transmission of plant single-stranded DNA viruses. Annu Rev Entomol. 2021;66:389–05.
7. Wang HL, Lei T, Wang XW, Cameron S, Navas-Castillo J, et al. A comprehensive framework for the delimitation of species within the *Bemisia tabaci* cryptic complex, a global pest-species group. Insect Sci. 2024;0:1–22.
8. Fiallo-Olivé E, Lett JM, Martin DP, Roumagnac P, Varsani A, Zerbini FM, Navas-Castillo J, ICTV Report Consortium. ICTV virus taxonomy profile: *Geminiviridae* 2021. J Gen Virol. 2021;102:001696.
9. Rojas MR, Hagen C, Lucas WJ, Gilbertson RL. Exploiting chinks in the plant's armor: evolution and emergence of geminiviruses. Annu Rev Phytopathol. 2005;43:361–94.
10. Hanley-Bowdoin L, Bejarano ER, Robertson D, Mansoor S. Geminiviruses: masters at redirecting and reprogramming plant processes. Nat Rev Microbiol. 2013;11(11):777–88.
11. Kamal H, Zafar MM, Razzaq A, Parvaiz A, Ercisli S, et al. Functional role of geminivirus encoded proteins in the host: past and present. Biotechnol J. 2024;19(6):e2300736.
12. Góngora-Castillo E, Ibarra-Laclette E, Trejo-Saavedra DL, Rivera-Bustamante RF. Transcriptome analysis of symptomatic and recovered leaves of geminivirus-infected pepper (*Capsicum annuum*). Virol J. 2012;9:295.
13. Pierce EJ, Rey MEC. Assessing global transcriptome changes in response to South African cassava mosaic virus [ZA-99] infection in susceptible *Arabidopsis thaliana*. PLoS ONE. 2013;8(6):e67534.
14. Allie F, Pierce EJ, Okoniewski MJ, Rey C. Transcriptional analysis of South African cassava mosaic virus-infected susceptible and tolerant landraces of cassava highlights differences in resistance, basal defense and cell wall associated genes during infection. BMC Genomics. 2014;15:1006.
15. Miozzi L, Napoli C, Sardo L, Accotto GP. Transcriptomics of the interaction between the monopartite phloem-limited geminivirus tomato yellow leaf curl Sardinia virus and *Solanum lycopersicum* highlights a role for plant hormones, autophagy and plant immune system fine tuning during infection. PLoS ONE. 2014;9(2):e89951.

16. Kushwaha N, Sahu PP, Prasad M, Chakraborty S. Chilli leaf curl virus infection highlights the differential expression of genes involved in protein homeostasis and defense in resistant Chilli plants. Appl Microbiol Biotechnol. 2015;99:4757–70.
17. Kushwaha NK. Chilli leaf curl virus infection downregulates the expression of the genes encoding chloroplast proteins and stress-related proteins. Physiol Mol Biol Plants. 2019;25(5):1185–96.
18. Wu MS, Ding X, Fu X, Lozano-Duran R. Transcriptional reprogramming caused by the geminivirus tomato yellow leaf curl virus in local or systemic infections in *Nicotiana Benthamiana*. BMC Genomics. 2019;20:542.
19. Song L, Wang Y, Zhao L, Zhao T. Transcriptome profiling unravels the involvement of phytohormones in tomato resistance to the tomato yellow leaf curl virus (TYLCV). Horticulturae. 2022;8:143.
20. Namgial T, Singh AK, Singh NP, Francis A, Chattopadhyay D, et al. Differential expression of genes during recovery of *Nicotiana tabacum* from tomato leaf curl Gujarat virus infection. Planta. 2023;258:37.
21. Romero-Rodríguez B, Petek M, Jiao C, Križnik M, Zagorščak M, et al. Transcriptional and epigenetic changes during tomato yellow leaf curl virus infection in tomato. BMC Plant Biol. 2023;23:651.
22. Jammes M, Golyaev V, Fuentes A, Laboureau N, Urbino C, et al. Transcriptome and small RNAome profiling uncovers how a recombinant begomovirus evades RDRγ-mediated silencing of viral genes and outcompetes its parental virus in mixed infection. PLoS Pathog. 2024;20(1):e1011941.
23. Nagendran KM, Mohankumar S, Aravintharaj R, Balaji CG, Manoranjitham SK, et al. The occurrence and distribution of major viruses infecting cucurbits in Tamil Nadu state, India. Crop Prot. 2017;99:10–6.
24. Wu HJ, Li M, Hong N, Peng B, Gu QS. Molecular and biological characterization of melon-infecting squash leaf curl China virus in China. J Integr Agr. 2020;19(2):570–77.
25. Qiu YH, Zhang HJ, Tian W, Fan LG, Du MX, et al. First Report of Squash Leaf Curl China Virus Infecting Tomato in China. Plant Dis. 2022;106(9):2539.
26. Pan LL, Chi Y, Liu C, Fan YY, Liu SS. Mutations in the coat protein of a begomovirus result in altered transmission by different species of whitefly vectors. Virus Evol. 2020;6(1):veaa014.
27. Kon T, Dolores LM, Bajet NB, Hase S, Takahashi H et al. Molecular characterization of a strain of squash leaf curl China virus from the Philippines. J Phytopathol. 2003;151(10).
28. Tahir M, Haider M, Briddon R. First report of Squash leaf curl China virus in Pakistan. Australas Plant Dis. 2010;5:21–4.
29. Chen YJ, Lai HC, Lin CC, Neoh ZY, Tsai WS. Genetic diversity, pathogenicity and pseudorecombination of cucurbit-infecting begomoviruses in Malaysia. Plants. 2021;10:2396.
30. Kamal H, Minhas FA, Farooq M, Tripathi D, Hamza M, et al. *Silico* prediction and validations of domains involved in *Gossypium hirsutum* SnRK1 protein interaction with cotton leaf curl Multan betasatellite encoded βC1. Front Plant Sci. 2019;10:656.
31. Breves SS, Silva FA, Euclydes NC, Saia TFF, Jean-Baptiste J et al. Begomovirus–host interactions: viral proteins orchestrating intra and intercellular transport of viral DNA while suppressing host defense mechanisms. Viruses. 2023;15;1593.
32. Stirbet A, Lazár D, Guo Y, Govindjee G. Photosynthesis: basics, history and modelling. Ann Bot-London. 2020;126:511–37.
33. Liu J, Yang J, Bi HP, Zhang P. Why mosaic? Gene expression profiling of African cassava mosaic virus-infected cassava reveals theeffect of chlorophyll degradation on symptom development. J Integr Plant Biol. 2014;56(2):122–32.
34. Bwalya J, Alazem M, Kim KH. Photosynthesis-related genes induce resistance against soybean mosaic virus: evidence for involvement of the RNA silencing pathway. Mol Plant Pathol. 2022;23(4):543–60.
35. Zhou JM, Zhang YL. Plant immunity: danger perception and signaling. Cell. 2020;181:978–89.
36. Zhang MM, Zhang SQ. Mitogen-activated protein kinase cascades in plant signaling. J Integr Plant Biol. 2022;64(2):301–41.

Publisher's note